

A View of Dynamics Changes in the Molten Globule-native Folding Step by Quasielastic Neutron Scattering

Zimei Bu^{1*}, Dan A. Neumann¹, Seung-Hun Lee¹, Craig M. Brown¹
Donald M. Engelman² and Charles C. Han¹

¹NIST Center for Neutron Research, and Polymers Division, National Institute of Standards and Technology Gaithersburg, MD 20899-8562, USA

²Department of Molecular Biophysics and Biochemistry Yale University, 266 Whitney Ave., New Haven, CT 06520-8114, USA

In order to understand the changes in protein dynamics that occur in the final stages of protein folding, we have used neutron scattering to probe the differences between a protein in its folded state and the molten globule states. The internal dynamics of bovine α -lactalbumin (BLA) and its molten globules (MBLA) have been examined using incoherent, quasielastic neutron scattering (IQNS). The IQNS results show length scale dependent, pico-second dynamics changes on length scales from 3.3 to 60 Å studied. On shorter-length scales, the non-exchangeable protons undergo jump motions over potential barriers, as those involved in side-chain rotamer changes. The mean potential barrier to local jump motions is higher in BLA than in MBLA, as might be expected. On longer length scales, the protons undergo spatially restricted diffusive motions with the diffusive motions being more restricted in BLA than in MBLA. Both BLA and MBLA have similar mean square amplitudes of high frequency motions comparable to the chemical bond vibrational motions. Bond vibrational motions thus do not change significantly upon folding. Interestingly, the quasielastic scattering intensities show pronounced maxima for both BLA and MBLA, suggesting that “clusters” of atoms are moving collectively within the proteins on picosecond time scales. The correlation length, or “the cluster size”, of such atom clusters moving collectively is dramatically reduced in the molten globules with the correlation length being 6.9 Å in MBLA shorter than that of 18 Å in BLA. Such collective motions may be important for the stability of the folded state, and may influence the protein folding pathways from the molten globules.

© 2000 Academic Press

Keywords: protein dynamics; protein folding dynamics; molten globule; quasielastic neutron scattering; α -lactalbumin

*Corresponding author

Introduction

Proteins can form collapsed, partially folded states under equilibrium and non-equilibrium conditions. Such partially folded states have been shown to resemble the kinetic folding intermediate states along the protein-folding pathway (Dill,

1990; Shortle, 1996; Dobson & Karplus, 1999). In addition to their roles in understanding the mechanisms of protein folding, partially folded proteins have also been shown to be important in cell functions (for a review, see Wright & Dyson, 1999). Besides structural and thermodynamic studies, dynamic information about a protein on different time and length scales is also necessary to gain insight into the mechanisms of the protein folding process. Studying the dynamics can provide us with information about the interaction potential energy landscape, which is the basis for understanding protein stability and rationalizing protein design (Guo & Thirumalai, 1996).

A molten globule is a partially folded protein that is compact with native-like secondary structure and overall backbone-folding topology, but lacks the extensive, specific side-chain packing

Abbreviations used: BLA, bovine α -lactalbumin; MBLA, bovine α -lactalbumin molten globule; A-MBLA, acid form of bovine α -lactalbumin molten globule at pH=3.0; N-MBLA, apo α -lactalbumin at neutral pH at 30°C; EISF, elastic incoherent structure factor; FWHM, full width at half maximum of a peak; IQNS, incoherent quasielastic neutron scattering; PSD, position-sensitive detector; SPINS TAS, spin-polarized triple-axis spectrometer; TOF, time-of-flight.

E-mail address of the corresponding author: zimei.bu@nist.gov

interactions of the native structure (for a review, see Ptitsyn (1995). Structural studies have shown that the side-chains in a molten globule are more disordered and can adopt a greater variety of conformations than in a native protein (Doig & Sternberg, 1995; Klefhaber *et al.*, 1995). Being able to form the tight and specific side-chain interactions typical of a native protein is considered to be the final and essential step in the protein-folding pathway (Levitt *et al.*, 1997). The packing process from a molten globule to the native protein is considered to be energetically more difficult than forming the collapsed, disordered folding intermediates (Levitt *et al.*, 1997; Ptitsyn, 1995). Many *de novo* designed proteins seem to lack the side-chain interactions of a native fold. A recent study has shown that molten globules preserve most of the native internal hydration sites and have native-like surface hydration (Denisov *et al.*, 1999). Nevertheless, little is known about the dynamics of this partially folded state.

The molten globule of α -lactalbumin, a small, calcium-binding protein (see Figure 1 for the native structure), is of particular interest for dynamics studies, since α -lactalbumin molten globule is a prototype for studying partially folded intermediates. A dynamics study can therefore be based on the intensive structural, thermodynamic, and kinetic studies on α -lactalbumin molten globules (Dobson, 1994; Kuwajima, 1996) to interpret the dynamics results. α -Lactalbumin forms a molten globule at low pH conditions, or in the absence of calcium ion at neutral pH at above 25 °C (Griko & Remeta, 1999). The formation of the molten globule is evidenced by a substantial loss of the near-ultraviolet circular dichroism signal and a significant reduction in NMR chemical shift dispersion, indicating that the side-chains are substantially disordered. Small angle X-ray scattering and dynamic light scattering have shown that the α -lactalbumin molten globules are compact under both equilibrium and kinetic conditions with the dimension of the molten globule expanded by about 9% relative to the native fold (Kataoka *et al.*, 1997; Gast *et al.*, 1998). The α -lactalbumin can form molten globules even in the absence of disulfide bonds (Redfield *et al.*, 1999). The structure of the α -lactalbumin molten globule is highly heterogeneous, having a structured α domain with some native-like packing interactions but an unstructured β domain and loop regions (Baum *et al.*, 1989; Alexandrescu *et al.*, 1993; Wu *et al.*, 1995; Peng & Kim, 1994; Peng *et al.*, 1995; Schulman *et al.*, 1997; Wu & Kim, 1998).

Neutron scattering offers a method to study the dynamics, with the advantage of measuring motions both on different time and length scales. There have been extensive applications of neutron scattering to the study of condensed matter dynamics, including small organic molecular crystals, polymers, and biological systems (Bee, 1988; Smith, 1991; Reat *et al.*, 1998; Zaccai, 2000). Quasi-elastic neutron scattering studies of the dynamics of

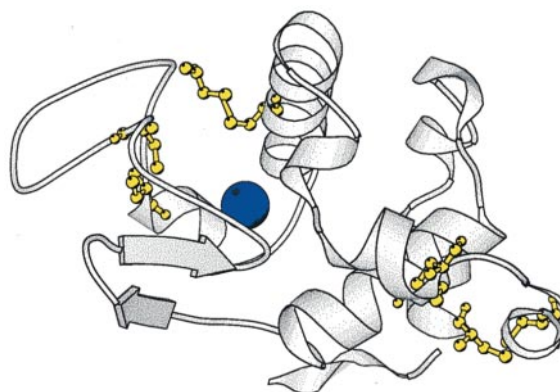


Figure 1. The native structure of α -lactalbumin has two domains, one is the α domain that consists largely of α -helices and the other one is the β domain that has a significant content of β -sheet (Pike *et al.*, 1996). α -Lactalbumin contains four disulfide bonds (in yellow), two in the α domain, one in the β domain and one cross-linking the two domains. The calcium ion (in blue) is located in the helix-turn-helix motif that spans the interface between the α and the β domains.

hydration water in proteins (Bellissent-Funel *et al.*, 1992), the dynamics of a denatured protein (Receveur *et al.*, 1997) and the truncated form of staphylococcal nuclease (Kataoka *et al.*, 1999) are reported. It is unfortunate that the opportunities and the quality of study have been limited by the scant availability of intense neutron sources and appropriate instrumentation.

Here, we report an incoherent quasielastic neutron scattering (IQNS) study of the internal dynamics of native fold of bovine α -lactalbumin (BLA) and two forms of the α -lactalbumin molten globules (MBLA), the acid form of BLA (A-MBLA) and the apo BLA at neutral pH at 30 °C (N-MBLA). IQNS of our study mainly measures the self-correlation function of the non-exchangeable protons of a protein dissolved in $^2\text{H}_2\text{O}$ on time scales of 10^{-10} to 10^{-13} seconds and on length scales between 3.3 to 60 Å. Since the non-exchangeable protons in the side-chains dominate the incoherent scattering, such experiments mainly probe changes in side-chain dynamics.

Our IQNS study reveals length scale-dependent, picosecond dynamics changes in the molten globules as compared to BLA. On longer length scales, the side-chain protons undergo spatially restricted diffusive motions with more restrictions to proton diffusion in the native protein than in the molten globules. On shorter length scales, dominated by local dynamics, the protons undergo local jump motions over potential barriers. The mean residence time for the protons to stay in a potential well is $\tau_{\text{BLA}} = 56(\pm 7)$ ps and $\tau_{\text{MBLA}} = 23(\pm 2)$ ps (where the errors are the standard deviations). The average height of the potential barrier to local jump motions is therefore lowered in the molten

globules. However, the root mean square jump distances are not changed within error with $\langle r^2 \rangle_{\text{BLA}}^{0.5} = 3.7(\pm 0.3) \text{ \AA}$ and $\langle r^2 \rangle_{\text{MBLA}}^{0.5} = 3.2(\pm 0.3) \text{ \AA}$, suggesting that the protons are involved in the rotamer changes. Both BLA and MBLA have indistinguishable mean square amplitudes of high frequency vibrations that are comparable to the chemical bond vibrational motions. High frequency, bond vibrational motions thus do not change significantly upon protein unfolding. By examining the maxima caused by the coherent component of the quasielastic intensity, we show that there are collective motions within both the native protein and the molten globules. The correlation length ξ for collective motions is longer in the native protein than in the molten globule with $\xi = 6.9(\pm 1.2) \text{ \AA}$ within the molten globules and $\xi = 18(\pm 4) \text{ \AA}$ within the native protein. Collective motions seen here may reduce the entropy cost of creating a folded protein. Our study also presents an experimental approach to sketch the energy landscape of protein folding in the native state and the partially folded states by dynamic neutron scattering.

The neutron-scattering functions

After striking a molecule, neutrons undergo changes both in the directions of travel and in energy. Structural and dynamic information can be obtained by studying the scattering intensity as a function of the magnitude of the neutron momentum transfer, $Q = 4\pi \sin(\theta)/\lambda$ and the neutron energy transfer $E = \hbar\omega$ (Bee, 1988; Higgins & Benoit, 1994), where 2θ is the scattering angle, λ is the wavelength and ω is the frequency of the neutrons. Molecular structures can be studied by elastic scattering intensity at different Q values at zero energy transfer, as in a neutron diffraction experiment. Different modes of macromolecule motions cause changes in frequencies or energy of the scattered neutrons, which is analogous to the Doppler effect. Slow motions on time scales between 10^{-9} to 10^{-12} seconds (such as the intra-molecular diffusive motions and the side-chain rotational motions of a macromolecule) give rise to quasielastic broadening of the elastic scattering peak at low energy transfer values (from 10^{-3} to 1 meV). High frequency motions, corresponding to time scales faster than 10^{-12} seconds (such as the vibrational motions of a chemical bond), can be studied by inelastic neutron scattering at higher energy transfer values (>10 meV).

In a quasielastic neutron scattering experiment, the measured quantity is the double-differential cross section, $\partial^2\sigma/\partial\Omega\partial\omega$, which is the probability a neutron scattered into the solid angle $\partial\Omega$ with a change in frequency $\partial\omega$:

$$\frac{\partial^2\sigma}{\partial\Omega\partial\omega} = N \frac{k_f}{k_i} \frac{1}{4\pi} [\sigma_{\text{inc}} S_{\text{inc}}(Q, \omega) + \sigma_{\text{coh}} S_{\text{coh}}(Q, \omega)] \quad (1)$$

where N is the number of nuclei; k_f and k_i are the

magnitudes of the final and the initial wave vectors, respectively; σ is the cross-section related to the scattering strength of the neutron by the nuclei. $S(Q, \omega)$ is the normalized scattering function that corresponds to the correlation function of the motion of the nuclei. The subscripts inc and coh correspond to the incoherent and coherent components, respectively.

The incoherent term $S_{\text{inc}}(Q, \omega)$ gives information about the self-correlation of the positions of the individual nucleus at different times. The coherent term $S_{\text{coh}}(Q, \omega)$ gives information about the correlation among positions of different nuclei at different times. A protein molecule contains a large amount of non-exchangeable protons that have a large incoherent scattering cross-section; about 87% of the total scattering is incoherent scattering from the non-exchangeable protons. Thus, incoherent scattering $S_{\text{inc}}(Q, \omega)$ from the protons of a protein dominates the scattering, and the self-correlation function of the protons is mainly measured.

The internal dynamics of a protein ranges from picoseconds to seconds (Karplus & McCammon, 1983). IQNS mainly measures the side-chain motions on the picosecond time scales (Higgins & Benoit, 1994) because side-chain protons dominate the scattering intensity; about 83% of the non-exchangeable protons are from the side-chains. The rotational and the translational motions of the whole protein and the protein backbone motions take tens of nanosecond to milliseconds. Although the scattering from such slow motions is quasielastic in nature, the correspondent neutron energy transfers are much narrower than the instrument energy resolution employed in this study, and their contributions to the broadening quasielastic scattering spectra can thus be ignored.

The incoherent, quasielastic scattering function is described as:

$$S_{\text{inc}}(Q, \omega) = \exp(-Q^2 \langle u^2 \rangle / 3) \times \left[A_0(Q) \delta(\omega) + \sum_{i=1}^n A_i(Q) L(\omega, \Gamma_i) \right] \quad (2)$$

assuming that the high-frequency, bond vibrational motions are not coupled to the quasielastic motions. In equation (2), $\langle u^2 \rangle$ is the mean square amplitude of vibrations; $A_0(Q) \delta(\omega)$ is the elastic term with an infinitely high spectrometer energy resolution $\delta(\omega)$; $\sum_{i=1}^n A_i(Q) L(\omega, \Gamma_i)$ is the quasielastic term that measures the mobility of the protons within the protein. For a spectrometer of finite energy resolution, the elastic line $\delta(\omega)$ is replaced by a Gaussian peak $R(Q, \omega)$ with the full width at half maximum of the Gaussian peak being the instrument energy resolution. The experimentally measured scattering function is that of equation (2) convoluted with the spectrometer resolution function as shown in equation (6).

The quasielastic term, $\Sigma_{i=1}^n A_i(Q)L(\omega, \Gamma_i)$, is a sum of Lorentzian functions:

$$L(\omega, \Gamma_i) = \frac{1}{\pi} \frac{\Gamma_i(Q)}{\Gamma_i(Q)^2 + \omega^2} \quad (3)$$

with Γ_i being the half width at half maximum of a Lorentzian peak. The magnitude of Γ_i is a measure of the mobility of the protons. Although the present study does not measure the inelastic scattering, the high frequency, vibrational motions produce the Q -dependent Debye-Waller factor $\exp(-Q^2\langle u^2 \rangle/3)$ in the total scattering intensity. The mean square amplitude of such vibrations ($\langle u^2 \rangle$) can be extracted from the Q dependence of the scattering intensity.

$A_o(Q)$ in equation (2) is the elastic incoherent structure factor (EISF) that corresponds to the time-averaged spatial distribution of the protons. EISF as a function of Q therefore gives information about the geometry of the motions. EISF also gives information about the fraction of "non-diffusive motion", f_{nd} , defined by the instrument energy resolution. The parameter f_{nd} can be obtained from $A_o(Q)$ (Bellissent-Funel *et al.*, 1992; Receveur *et al.*, 1997; see equation (4) and Figure 5).

Results

Figure 2 gives the two-dimensional quasielastic neutron scattering spectra, $S(Q, \omega)$, measured as a function of the momentum transfer Q and the energy transfer $\hbar\omega$. Figure 2(a) and (b) show that both N-MBLA and A-MBLA have broader quasielastic spectra (with respect to energy transfer) than BLA within the dynamic range measured (≥ 0.065 meV on TOF and ≥ 0.085 meV on SPINS TAS). A broader quasielastic peak indicates that the side-chains within the molten globules are more mobile than within the native protein. The half width at half maximum of the quasielastic, Lorentzian component Γ and the EISF can be obtained by fitting the experimental data to equation (6) as shown in Figure 3. Information about the nature of the motions can be obtained by interpreting the Q dependence of Γ and EISF.

Although the quasielastic spectra of BLA/N-MBLA (Figure 2(a)) and BLA/A-MBLA (Figure 2(b)) were collected on different spectrometers of slightly different instrument energy resolutions (see Materials and Methods), the Q dependence of Γ and the magnitude of Γ of A-MBLA and N-MBLA are similar. We select the data of N-MBLA collected from the TOF spectrometer (of a better instrument energy resolution and better signal-to-noise ratio) to describe the dynamics differences of molten globules from the native state. On the other hand, since the SPINS TAS employs a single detector to cover the different Q values, the technical problem of detector non-uniformity was eliminated. We therefore use the data collected on SPINS TAS from A-

MBLA to describe the Q dependence of the quasielastic scattering intensity, as shown in Figure 6.

Spatially restricted long-range diffusive motion and local jump motions within the proteins, show less restriction of motions in the molten globules

Figure 4 plots Γ of N-MBLA as a function of Q . The Γ of N-MBLA varies more with Q than that of BLA. For both BLA and MBLA, the Q dependence of Γ can be described as having two regions. At $Q \leq 1.0 \text{ \AA}^{-1}$ for BLA and $Q \leq 1.5 \text{ \AA}^{-1}$ for MBLA, Γ increases with Q . At high Q values, Γ shows a plateau region in which Γ is nearly Q independent. For both BLA and MBLA, a fit of Γ versus Q^2 in the Q dependent region does not give zero intercepts, suggesting that the protons do not undergo free, translational diffusion. Such features are typical of spatially constrained diffusive motion (Bee, 1988; Higgins & Benoit, 1994).

A model of "diffusion within a spherical potential plus local jump motions" (Bee, 1988; Volino & Dianoux, 1980) was used to describe such a Γ dependence on Q . The sphere represents the spatial constraints imposed on a proton by its environment. The diffusion within a sphere model has been used by Bellissent-Funel *et al.* (1992) to study the dynamics of hydration water within a protein, and by Receveur *et al.* (1997) to study the dynamics changes upon the denaturation of yeast phosphoglycerate kinase.

The radius of the spherical potential can be estimated from the EISF (Figure 5). The experimentally measured EISF contains two terms, see equation (4) (Bellissent-Funel *et al.*, 1992; Receveur *et al.*, 1997). One term is the fraction of the "immobile" hydrogen atoms (f_{nd}) as "seen" by the TOF spectrometer due to the finite energy resolution of the instrument. The other term is the fraction of a time-averaged distribution of protons ($1 - f_{nd}$) diffusing within a sphere of radius of R :

$$A_o(Q) = f_{nd} + (1 - f_{nd}) \frac{9}{(QR)^6} \times [\sin(QR) - QR \cos(QR)]^2 \quad (4)$$

From Figure 5 and equation (4) we obtained the radii of the spheres $R_{BLA} = 4.1(\pm 0.1) \text{ \AA}$ and $R_{N-MBLA} = 5.4(\pm 0.1) \text{ \AA}$, which reflects reduced constraints to proton motion in N-MBLA. Although a better fit to the EISF was achieved by including two spheres in the EISF analysis (see Figure 5), we present the results with the one sphere model to demonstrate a lessened constraint to the diffusive motion of protons within N-MBLA. Similar values of the radius of R of the spherical potential can also be obtained from the formula $QR \approx \pi$ (Volino & Dianoux, 1980) in the low Q value region ($Q < 0.5 \text{ \AA}^{-1}$ in Figure 4) although the uncertainty in R obtained by this method is higher than that

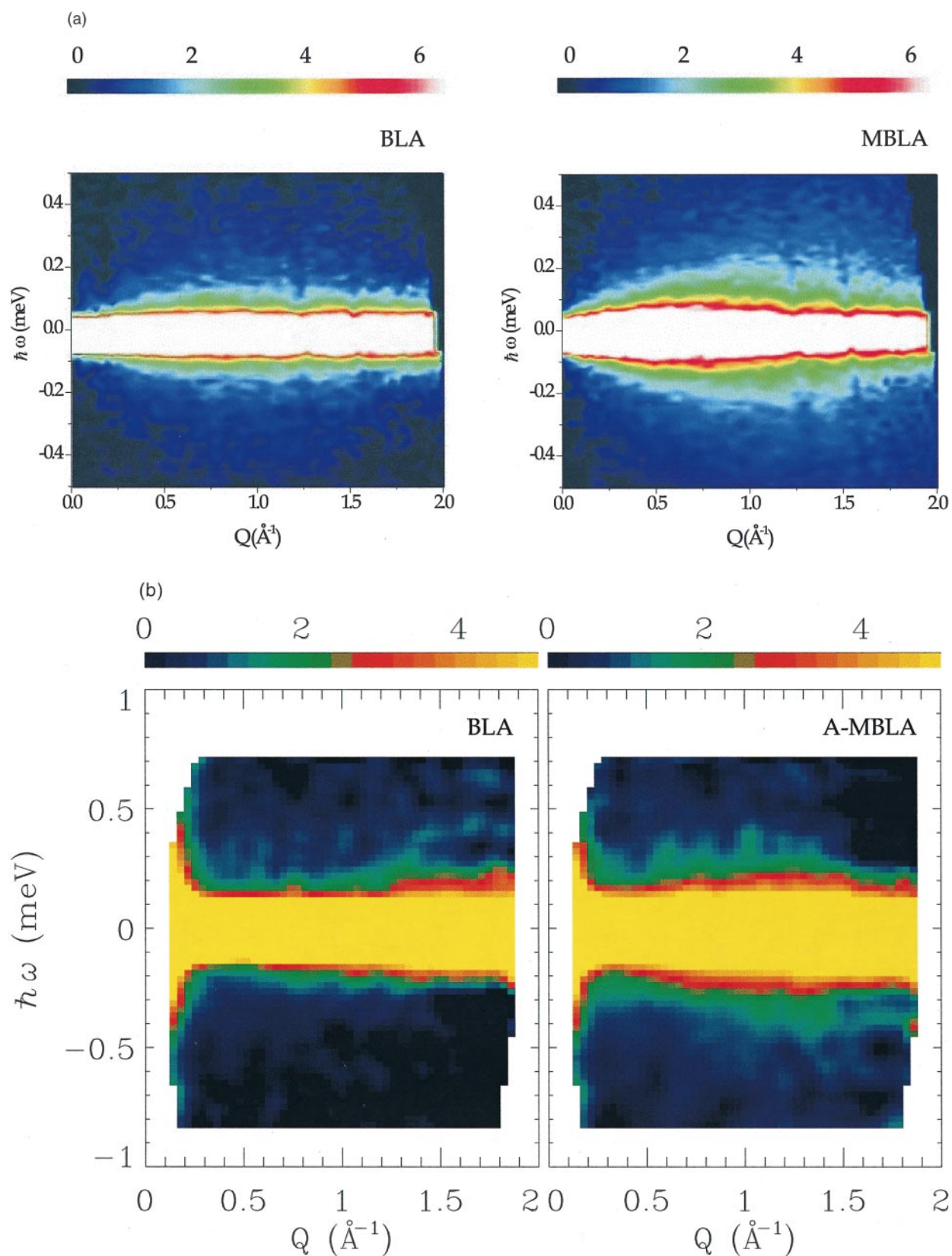


Figure 2. Two dimensional quasielastic neutron scattering spectra $S(Q, \omega)$ (in arbitrary unit) versus $\hbar\omega$ and Q of (a) BLA in 20 mM Tris- d_{11} , $p^2H = 8.0$ at 30°C , and N-MBLA in 20 mM Tris- d_{11} , $p^2H = 8.0$ at 30°C ; (b) BLA in 20 mM Tris- d_{11} , $p^2H = 8.0$ at 30°C and, and A-MBLA in 20 mM glycine- d_5 , ^2HCl , $p^2H = 3.0$ at 30°C . The data in (a) were collected on TOF, and the data in (b) were collected on SPINS TAS.

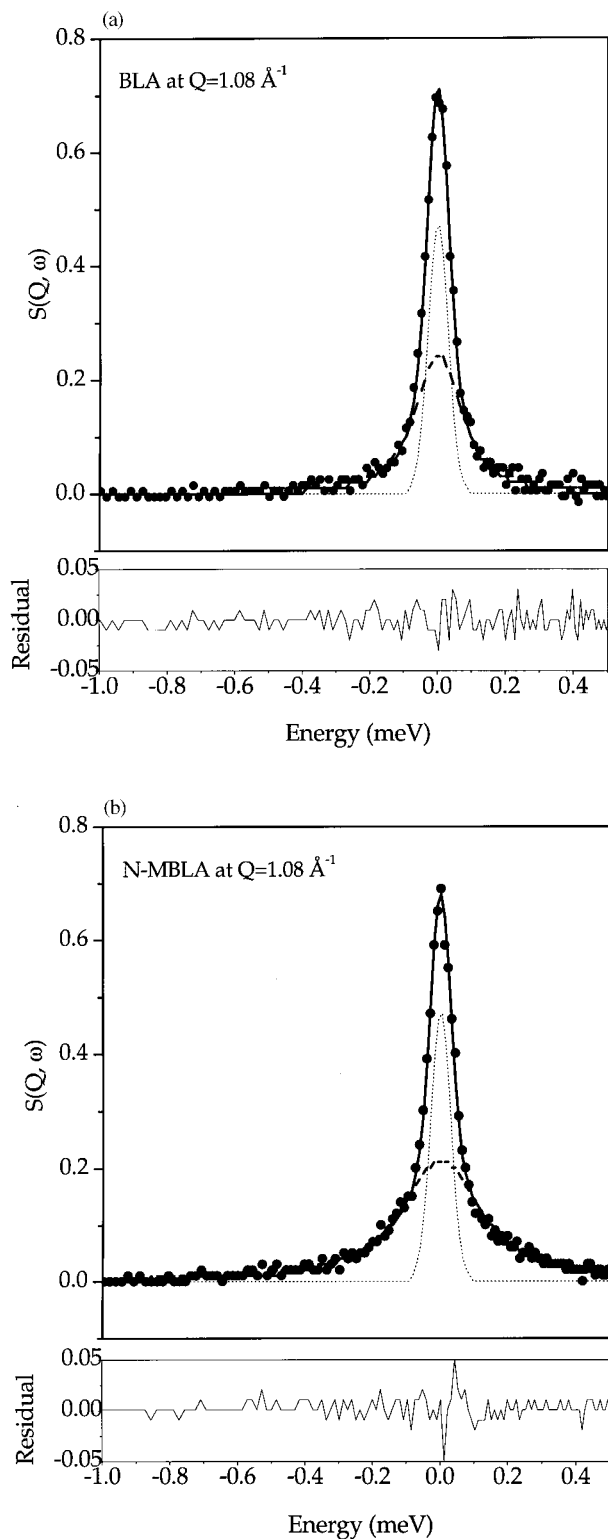


Figure 3. Quasielastic neutron scattering spectra $S(Q, \omega)$ (in arbitrary unit) at $Q = 1.08 \text{ \AA}^{-1}$ obtained from TOF of (a) BLA at 20 mM Tris- d_{11} , $p^2H = 8.0$ and 30°C and (b) N-MBLA (apo-BLA at 20 mM Tris- d_{11} , $p^2H = 8.0$ and 30°C). Experimental data (\bullet). The experimental data are fit by equation (6). The dashed lines are the quasielastic component $L(\omega, \Gamma)$ which is a Lorentzian peak, the broken lines are the Gaussian peak $R(Q, \omega)$ representing the instrument resolution, and the continuous lines are the total fit (Gaussian peak plus the

obtained by equation (4) and Figure 5, considering the few data points used in fitting.

According to the spherical potential model, the diffusion constant D within a sphere of radius R can be calculated as $\Gamma = 4.333D/R^2$ in the $QR \leq \pi$ region. The diffusion constants are: $D_{\text{BLA}} = (4.2(\pm 0.5)) \times 10^{-6} \text{ cm}^2/\text{s}$ and $D_{\text{N-MBLA}} = (7.3(\pm 0.8)) \times 10^{-6} \text{ cm}^2/\text{s}$. The larger proton diffusion constant in MBLA reflects reduced restrictions to diffusive motion within the molten globule than within the native protein.

In the high Q region, one observes motion on short length scales ($Q \geq 1 \text{ \AA}^{-1}$ corresponding to 6.3 \AA for BLA, and $Q \geq 1.4 \text{ \AA}^{-1}$ corresponding to 4.4 \AA for N-MBLA). On such short-length scales, local-jump motions of the protons become important. The local-jump motion is related to the local potential energy barrier imposed on a proton by its neighbors. The distance of each jump step can be approximated as the width of the potential well. The mean residence time of a hydrogen atom in a potential well before it jumps to another potential well is $\tau = 1/\Gamma$ with Γ obtained from the high Q region where Γ is nearly Q independent. The mean residence time of the non-exchangeable protons in a potential well is $\tau_{\text{BLA}} = 56(\pm 7) \text{ ps}$ for BLA, comparable to that of a small organic crystal norbornane (Bee, 1988, 1992). For N-MBLA the mean residence time is $\tau_{\text{N-MBLA}} = 23(\pm 2) \text{ ps}$, shorter than that of BLA.

The height of the potential barrier is related to the residence time by the Arrhenius relation:

$$\tau = \tau_0 \exp(E_a/k_B T) \quad (5)$$

where τ_0 is related to the torsional frequency, k_B is the Boltzmann constant, and E_a is the mean activation energy that is a measure of the mean height of the barrier. Although a temperature-dependent study is needed to measure the absolute value of E_a , the difference $\Delta E_a = k_B T \ln(\tau_{\text{N-MBLA}}/\tau_{\text{BLA}})$ between BLA and MBLA can be estimated by assuming τ_0 to be unchanged in the N-MBLA. The calculated ΔE_a at 303 K is $-2.24 \text{ kJ mol}^{-1}$ (or $-0.54 \text{ kcal mol}^{-1}$). The derived r.m.s.d. between two successive jumps $\langle r^2 \rangle^{0.5} = 6D\tau$ are similar for BLA and N-MBLA, with $\langle r^2 \rangle_{\text{BLA}}^{0.5} = 3.7(\pm 0.3) \text{ \AA}$ and $\langle r^2 \rangle_{\text{N-MBLA}}^{0.5} = 3.2(\pm 0.2) \text{ \AA}$. The change in residence time but not in the jump distance in N-MBLA indicates the rotational nature of the side-chain protons in sampling a distribution of rotamers.

Lorentzian peak) to the experimental data. The residuals of fit are presented as another panel at the bottom of the plot.

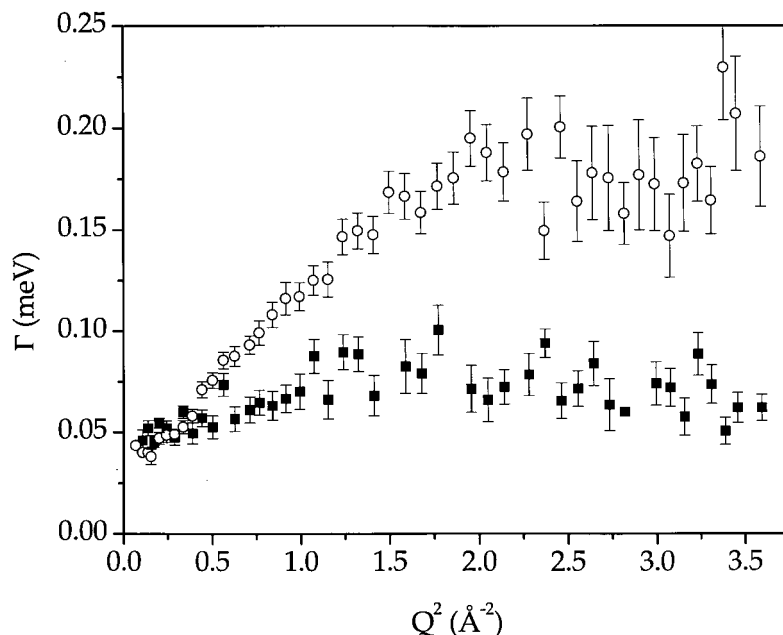


Figure 4. Q dependence of half-width at half-maximum Γ of the quasielastic Lorentzian peak of: BLA (■) and N-MBLA (○). Γ reflects the decay rate of the self-correlation function and is a measure of the mobility of the protons within the protein.

Collective diffusive motions within the protein, with a longer correlation length within the native protein

From the above analysis, we have derived information on non-localized but restricted diffusive motions of protons within the proteins. Restricted and non-localized motions indicate correlated motions within the protein (Bee, 1988; Donati *et al.*, 1999). There are two features to define correlated motions. One feature is that the microscopic motion steps of individual protons are correlated. This is apparent in Figure 4. At high Q values

where local dynamics are important, the Γ values of both BLA and MBLA are almost independent of the length scale of observation, which suggests that one step of the proton jump motion is correlated with (or “remembers”) the direction and magnitude of its previous jumps. At lower Q values, on longer length scales, one starts to observe a loss of correlation as Γ starts to become dependent on Q at a certain Q value, Q_{dc} . In the native protein, we observe such a loss of correlation of motions on longer length scales than in the molten globule with $Q_{dc} = 1.05 \text{ \AA}^{-1}$ for BLA and $Q_{dc} = 1.4 \text{ \AA}^{-1}$ for MBLA. The other feature of the correlated motion

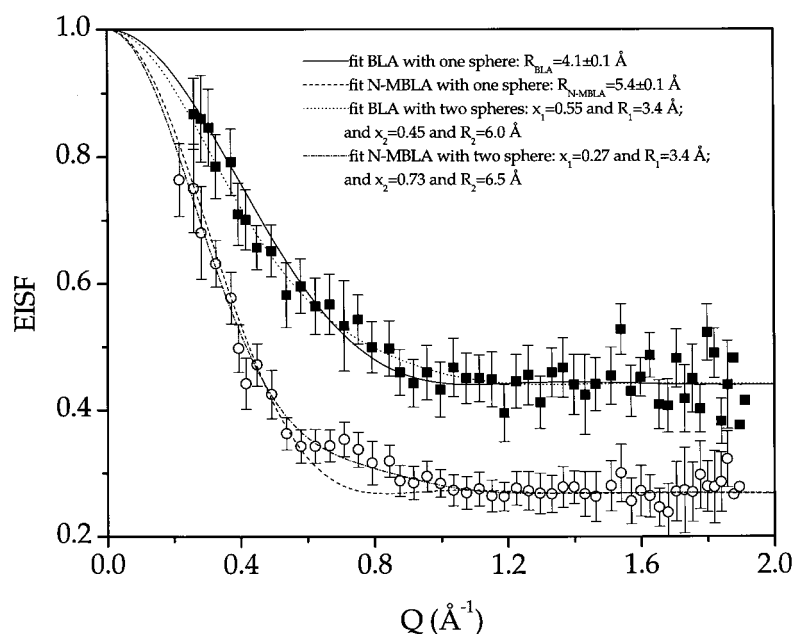


Figure 5. EISF of: BLA (■) and N-MBLA (○). Although a better fit to the EISF was achieved with a two-sphere model, we use the one-sphere model (equation (4)) to describe the change in the radius of the restriction potential to motion.

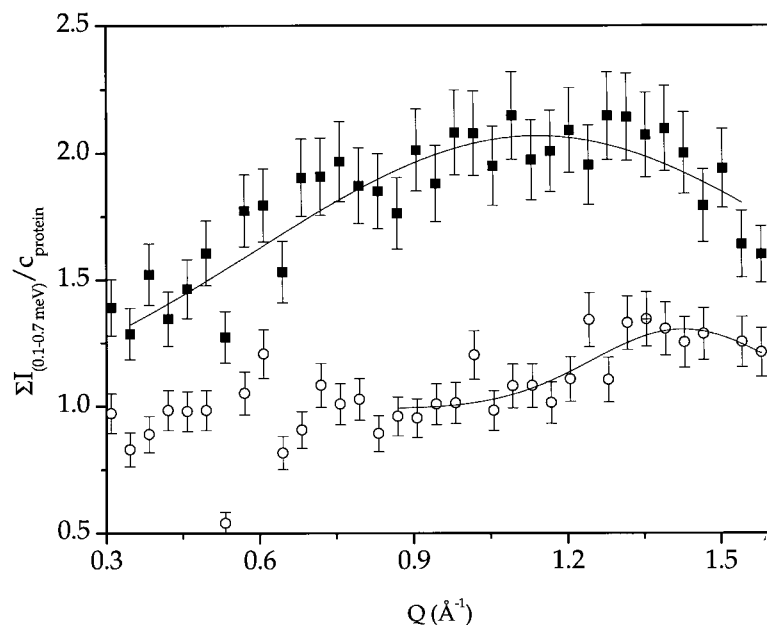


Figure 6. The quasielastic scattering intensity of: BLA (■) and A-MBLA (○) as a function of Q . The quasielastic scattering intensities were normalized by the protein concentrations. The data were obtained from SPINS TAS where a single detector was employed to cover the Q range studied, so that changes in intensity caused by detector non-uniformity at different Q are eliminated.

is the collective motion of different atoms. Collective motions within a native protein are assumed to be necessary for a fluctuating protein to maintain its structure and stability (Karplus & McCammon, 1983), and collective motions have been identified in molecular dynamics simulations (Ichiye & Karplus, 1991).

The quasielastic scattering intensity can reveal features of collective motions when such collective motions are prominent in affecting the properties of the total scattering intensity, since about 13% of the total quasielastic scattering intensity from a protein is coherent scattering. If only incoherent scattering is present, the total scattering intensity is Q -independent (Higgins & Benoit, 1994). Otherwise, when properties related to coherent scattering is apparent, the total scattering intensity shown in equation (1) depends on Q . This is evident from Figure 2(a) and (b) in which the total scattering intensity first decreases with increasing Q at low Q values (when $Q \leq 0.5 \text{\AA}^{-1}$), then increases with increasing Q to generate a maximum at $Q_{\text{max, A-MBLA}} = 1.1 \text{\AA}^{-1}$ for MBLA and $Q_{\text{max, BLA}} = 1.4 \text{\AA}^{-1}$ for BLA.

The maximum of the quasielastic intensity is generated by the correlation of a cluster of atoms moving collectively at a distance (d) apart corresponding to $d = 2\pi/Q_{\text{max}}$ (see Figures 2 and 6). The size, or the correlation length ξ , of such an atomic cluster moving collectively can be given by the full width at half maximum (FWHM) of the maximum, $\xi = 2\pi/\text{FWHM}$. Such a dynamic correlation is analogous to the static correlation in a neutron diffraction experiment. When there is a static correlation of the positions of the different atoms at a distance ($d_s = 2\pi/Q_{\text{max}}$) apart, a diffraction peak is generated by the elastic coherent scattering component. When such a static correlation is over a large

length scale (ξ_s) as in crystalline materials, a sharp diffraction peak is generated. The static correlation length can be obtained from the width of the diffraction peak by $\xi_s = 2\pi/\text{FWHM}$. In a static neutron diffraction experiment, incoherent scattering contributes only as a flat background that is independent of Q .

Figure 6 is the total quasielastic intensity as a function of Q by summing all the non-elastic scattering intensity in Figure 2. Figure 6 reproduces the maxima at $Q_{\text{max, A-MBLA}} = 1.1 \text{\AA}^{-1}$ and $Q_{\text{max, BLA}} = 1.4 \text{\AA}^{-1}$ in Figure 2. The maxima suggest that the motions of those atoms at $d_{\text{A-MBLA}} = 5.6(\pm 0.1) \text{\AA}$ and $d_{\text{BLA}} = 4.4(\pm 1.3) \text{\AA}$ distances apart within the proteins are moving "in phase". The correlation length, related to the size of a "cluster" of such atoms moving collectively, can be obtained from the FWHM of the maximum by fitting the experimental data to a Gaussian peak with $\xi = 2\pi/\text{FWHM}$. In analysis, Figure 6 shows that the correlation length of the collective motion is $\xi_{\text{MBLA}} = 6.9(\pm 1.2) \text{\AA}$ and $\xi_{\text{BLA}} = 18(\pm 4) \text{\AA}$. Slower collective motions on a longer-length scale within the native protein are highly possible. However, such slow motions cannot be probed with the instrument energy resolution employed in the present study, and await quasielastic scattering experiments with higher instrument energy resolution.

High-frequency vibrations do not change significantly in protein folding

The mean square vibration amplitude ($\langle u^2 \rangle$) related to the Debye-Waller factor can be obtained from a linear fit of $\ln I_{\text{total}}$ versus Q^2 as shown in equations (2) and (6). BLA and N-MBLA have similar $\langle u^2 \rangle$ values within error with $\langle u^2 \rangle_{\text{BLA}} = 0.51(\pm 0.09) \text{\AA}^2$ and $\langle u^2 \rangle_{\text{MBLA}} = 0.48(\pm 0.06) \text{\AA}^2$. The entropy change from native to

molten globule due to the high frequency, bond vibrational motions can be calculated as:

$$\Delta S_{\text{HF}} = k_{\text{B}}T \ln\left(\frac{\langle u^2 \rangle_{\text{MBLA}}}{\langle u^2 \rangle_{\text{BLA}}}\right)$$

The similar $\langle u^2 \rangle$ values of BLA and MBLA suggest that the high-frequency, vibrational motions do not contribute significantly to entropy changes in protein folding as discussed by Karplus *et al.* (1987); Doig & Sternberg (1995) and Brady & Sharp (1997).

Discussion

A native structure is considered to be at its global free energy minimum (Ptitsyn, 1995) unless a protein co-folds with another protein or has post-translational modifications. The side-chains are more disordered in the molten globules and a molten globule to native transition experiences an unfavorable loss in entropy that can be compensated by establishing the favorable interactions within the native protein. Besides such thermodynamics arguments, our IQNS results show that more restrictions to long range diffusive motions and a higher energy barrier to local jump motions within the native protein are features of the native structure in the global energy minimum.

The IQNS results show that the local jump rate of protons hopping over potential barrier within BLA is comparable to that of the small organic crystals (Bee, 1988, 1992). Our dynamics results thus support the structural analysis that a native protein is as densely packed as small organic crystals (Richards, 1977; Richards & Lim, 1993). However, unlike a small organic crystal, there is long-range and collective diffusive motion within the native protein. Collective motions are inferred from recent bioinformatic studies of protein families (Lockless & Ranganathan, 1999). Molecular dynamics simulations have also suggested such diffusive motions combined with hopping motions on the picosecond time scale within a protein to describe the kinetics of internal, collective motions of proteins (Amadei *et al.*, 1999). Long-range diffusive motions may facilitate the conformation flexibility of a protein that is important for binding and functions, and for tolerating amino acid residue substitutions (Matthews, 1995). Collective motions are probably responsible for the high-resolution structural observations that groups of linked atoms through small changes in torsion angles can relax strains within a protein (Liu *et al.*, 2000).

Studies show that the structures of molten globules are highly heterogeneous (Baum *et al.*, 1989; Alexandrescu *et al.*, 1993; Wu *et al.*, 1995; Peng & Kim, 1994; Peng *et al.*, 1995; Schulman *et al.*, 1997; Wu & Kim, 1998), indicating that the transitions either from molten globule to native or from molten globule to the more denatured states may not be all-to-none processes (Makhatadze & Privalov, 1995). Such a structural heterogeneity is reflected in the dynamics of MBLA. The fraction of non-dif-

fusive motion f_{nd} can be determined from the non-zero baselines of EISF in Figure 5 to be 0.44 for BLA and 0.27 for MBLA, respectively. About 27% of the protons in the molten globule are "non-difusive" on the time scale measured by TOF spectrometer. Since about 17% of the 743 non-exchangeable hydrogen atoms are on the backbone and assuming their slow motions are immobile, the remaining 10% immobile protons are from the side-chains in MBLA. A recent NMR experiment has revealed that the side-chain dynamics are highly heterogeneous on microsecond to millisecond time scales (Bai *et al.*, 2000).

Glass transition theories have been employed to formulate protein-folding reaction theories (Bryngelson & Wolynes, 1987, 1989). The IQNS results show features of the dynamics of glass-forming liquids. Toward the glass transition, a glass forming liquid experiences a growing spatial correlation of particle displacements (Donati *et al.*, 1999). Comparing the Γ versus Q^2 plot of BLA and MBLA (Figure 4), we observe a spatially correlated motion of the individual protons on a longer length scale in the native protein than in the molten globule. The maximum of the quasielastic intensity as a function of Q of MBLA in Figure 6 suggests that the motions of a cluster of atoms are spatially correlated. Such a growing range of cooperative motion is thought to be responsible for the dramatic change in dynamic properties toward glass transition of glass-forming liquids (Adam & Gibbs, 1965). A vibrational Raman optical activity study has shown that the native-like tertiary fold in molten globule α -lactalbumin is controlled by a continuous phase transition but not a first-order phase transition (Wilson *et al.*, 1996), indicating that structurally the α -lactalbumin molten globule to native transition can be comparable to glass transition experimentally. We propose that a growing spatially correlated motion within a partially folded protein may assist the molten globule to native transition. The development of collective motions within the molten globule seen here thus supports the view that the entropic cost of creating a folded protein is reduced by such motions.

Conclusion

The final stage of protein folding involves the formation of the specific side-chain packing that is characteristic of a native protein, but little is known about how such specific packing is achieved from the disordered side-chains in the collapsed, partially folded intermediates. We have used incoherent quasielastic neutron scattering to probe the change in dynamics of α -lactalbumin in its folded and the molten globule forms.

Changes in the picosecond time scale motions have been identified in the molten globules as compared to the native protein. These changes include long-range restricted diffusive motions and local jump motions. There are more restrictions to both

long-range, diffusive motions and local-jump motions within the native protein to help maintaining the native structure, besides the delicate balance of thermodynamic factors. Long-range diffusive motions within a native protein facilitate the conformation flexibility that is important for binding and functions, and to maintain stability. The mean square amplitudes of high frequency, bond vibrational motions do not change upon protein unfolding. The length scale-dependent, picosecond dynamics of BLA and MBLA reflects a portion of the hierarchy structure of the energy landscape within a protein (Frauenfelder *et al.*, 1991).

We have demonstrated the presence of collective motions on picosecond time scale within the molten globule. Progressively growing long range, collective motions may be important for the molten globule to native transition by reducing the entropy cost of creating a defined, native structure.

Materials and Methods

Sample preparation

Bovine α -lactalbumin (BLA) was purchased from Worthington Biochemical Co. (Newark, NJ, USA). Deuterium oxide (^2H , 99.9%) was purchased from Cambridge Isotope Laboratories, Inc (Andover, MA, USA). The protein was first dialyzed in H_2O to remove possible residual $(\text{NH}_4)_2\text{SO}_4$ in the sample. The purity of the protein was above 95% as judged from SDS-PAGE. The molten globules were prepared from apo α -lactalbumin. Apo α -lactalbumin was prepared as described (Griko & Remeta, 1999; Kataoka *et al.*, 1997). At 20 mM Tris-HCl (pH 8.0), apo bovine α -lactalbumin adopts a native-like molten globule form at above 25°C (Griko & Remeta, 1999; Kataoka *et al.*, 1997). We use this apo form of bovine α -lactalbumin at 30°C as one form of MBLA. The acid form of α -lactalbumin molten globule, A-MBLA was prepared by dissolving the apo bovine α -lactalbumin in 20 mM glycine- d_5 , ^2HCl , $\text{p}^2\text{H} = 3.0$, $^2\text{H}_2\text{O}$ buffer.

Before the neutron scattering experiments, the proteins were dissolved in $^2\text{H}_2\text{O}$ and lyophilized for four rounds to replace the exchangeable protons with deuterium. Protein concentration was determined by ultraviolet absorbance at 280 nm using 1.96 as the absorbance of 1 mg/ml of protein solution by dilution the protein $^2\text{H}_2\text{O}$ solution 100-200 times with H_2O buffer. The BLA and MBLA solutions were prepared by dissolving deuterium exchanged, proteins in 20 mM deuterated Tris- d_{11} - ^2HCl $^2\text{H}_2\text{O}$ (p^2H 8.0) buffer at 73.6 mg/ml and 74.7 mg/ml, respectively. A 20 mM Tris- d_{11} - ^2HCl (p^2H 8.0) $^2\text{H}_2\text{O}$ solution was used for background subtraction for both BLA and MBLA. No protein aggregations were present in the above $^2\text{H}_2\text{O}$ buffer solutions for protein concentrations up to 10 mg/ml for either BLA or MBLA as examined by solution small-angle X-ray scattering. No protein degradation was observed after the neutron scattering measurements as examined by an overloaded SDS-PAGE.

Quasielastic neutron scattering experiment

Quasielastic neutron scattering experiments were performed at the Fermi-Chopper Time-of-Flight Spec-

trometer (TOF) (Copley & Udovic, 1993) and at the SPINS Triple-Axis Spectrometer (TAS) at National Institute of Standards and Technology Center for Neutron Research (NIST NCNR). The incident neutron wavelength was 6.0 Å at TOF. The instrument energy resolution $R(Q, \omega)$ was determined from the elastic peak of vanadium of the same geometry as the sample, with the energy resolution FWHM at $Q = 0.3 \text{ \AA}^{-1}$ being 0.065 meV. The elastic momentum transfer range was $(0.3 < Q < 1.9) \text{ \AA}^{-1}$.

At SPINS TAS, we utilized a position-sensitive detector (PSD) in conjunction with a flat multi-crystal analyzer that increases the data collection rate by measuring the scattering at several energy and momentum transfers simultaneously. The incident neutron wavelength was 5.0 Å at SPINS TAS. The energy range of the scattered neutrons that are collected by the flat analyzer was 2.6 meV $< E_f < 3.7$ meV. By changing the incident energy and the scattering angle, we can survey the energy and momentum transfer $\hbar\omega - Q$ space. The energy transfer range varied from 0.085 meV to 0.8 meV, and the momentum transfer range varied from 0.08 \AA^{-1} to 2 \AA^{-1} with the momentum transfer resolution of about 0.02 \AA^{-1} .

The samples were loaded in a 0.8 mm thick aluminum annulus of $(20 \times 100) \text{ mm}^2$ for measurements. The fraction of the incident neutrons removed from the beam after passing through the sample $f = 1 - \exp(-N\sigma_T t)$ was calculated to be about 10%, where σ_T is the sum of coherent, incoherent and the absorption cross-sections of the sample, N the number of scattering unit per unit volume and t is the thickness of the sample (Windsor, 1981). No corrections for absorption and multiple scattering were therefore performed. The detector efficiency was calibrated by measuring the intensity in a vanadium elastic peak. Data were collected for about 48 hours for protein solutions and the buffer background, respectively. Measurements were at 30°C.

Data analysis

The scattering from the protein was obtained by subtracting the buffer scattering from the protein solution scattering, taking into account the solvent excluded volume:

$$S = S_s - S_b \frac{n_s}{n_b} (1 - \phi_2)$$

where S_s and S_b are the raw scattering data of the protein solution and the buffer background, respectively; n_s and n_b are the total neutron counts for the protein solution and the buffer before the sample, respectively; ϕ_2 is the volume fraction of the protein calculated from the protein concentration with the partial specific volume of the protein being 0.709 g/ml (Hendrix *et al.*, 1996) for both the native protein and the molten globule. The reduction in the bulk solvent mobility due to the presence of protein was estimated by $D_1/D_0 = 1/(1 + \phi_2/2)$ (Duval *et al.*, 1999) to be less than 0.97 at the protein concentrations measured, and was not considered when reducing data. After correction for the buffer background and detector efficiency, the experimentally measured scattering function is that of equation (2) convoluted with the spectrometer resolution function $R(Q, \omega)$:

$$S_{\text{inc}}(Q, \omega) = \exp(-Q^2 \langle u^2 \rangle / 3) [A_0(Q)R(Q, \omega) + (1 - A_0(Q))L(\omega, \Gamma) \otimes R(Q, \omega)] + B_0 + B_1\omega \quad (6)$$

where $B_0 + B_1\omega$ is the baseline for fitting the peaks. The $S_{\text{inc}}(Q, \omega)$ of both BLA and MBLA could be fit reasonably well by a single Lorentzian function (see Figure 3).

Acknowledgments

We thank John J. Rush for his enthusiastic support and advice, Taner Yildirim for making his TOF data analysis software available to us. We acknowledge the support of the National Institute of Standards and Technology, U. S. Department of Commerce, in providing the neutron facilities used in this work. The SPINS spectrometer is supported by the National Science Foundation under Agreement No. DMR-9986442. Z.B. thanks Samuel F. Trevino, Chun K. Loong, and Alan Nakatani for helpful discussions; and Paul Butler, William Russ and Alessandro Senes for critically reading the manuscript. D.M.E. thanks the NIH (GM 22778) for support.

References

- Adam, G. & Gibbs, J. H. (1965). On the temperature dependence of cooperative relaxation properties in glass-forming liquids. *J. Chem. Phys.* **43**, 139.
- Alexandrescu, A. T., Evans, P. A., Pitkeathly, M., Baum, J. & Dobson, C. M. (1993). Structure and dynamics of the acid-denatured molten globule state of alpha-lactalbumin: a two-dimensional NMR study. *Biochemistry*, **32**, 1707-1718.
- Amadei, A., de Groot, B. L., Ceruso, M. A., Paci, M., Di Nola, A. & Berendsen, H. J. (1999). A kinetic model for the internal motions of proteins: diffusion between multiple harmonic wells. *Proteins: Struct. Funct. Genet.* **35**, 283-292.
- Bai, P., Luo, L. & Peng, Z.-Y. (2000). Side-chain accessibility and dynamics in the molten globule state of alpha-lactalbumin: a 19F-NMR study. *Biochemistry*, **39**, 372-380.
- Baum, J., Dobson, C. M., Evans, P. A. & Hanley, C. (1989). Characterization of a partly folded protein by NMR methods: studies on the molten globule state of guinea pig alpha-lactalbumin. *Biochemistry*, **28**, 7-13.
- Bee, M. (1988). *Quasielastic Neutron Scattering, Principles and Applications in Solid State Chemistry, Biology and Materials Science*, Adam Hilger/Bristol and Philadelphia.
- Bee, M. (1992). Neutron investigation of reorientations in organic molecular compounds. *Spectrochim. Acta*, **48A**, 429-453.
- Bellissent-Funel, M. C., Teixeira, J., Bradley, K. & Chen, S. (1992). Dynamics of hydration water in protein. *J. Phys. I*, **2**, 995.
- Brady, G. P. & Sharp, K. A. (1997). Entropy in protein folding and in protein-protein interactions. *Curr. Opin. Struct. Biol.* **7**, 215-221.
- Bryngelson, J. D. & Wolynes, P. G. (1987). Spin glasses and the statistical mechanics of protein folding. *Proc. Natl Acad. Sci. USA*, **84**, 7524-7528.
- Bryngelson, J. D. & Wolynes, P. G. (1989). Intermediates and barrier crossing in a random energy model (with applications to protein folding). *J. Phys. Chem.* **93**, 6902-6915.
- Copley, J. & Udovic, T. (1993). Neutron time-of-flight spectroscopy. *J. Res. Natl Inst. Stand. Technol.* **98**, 71-87.
- Denisov, V. P., Jonsson, B. H. & Halle, B. (1999). Hydration of denatured and molten globule proteins. *Nature Struct. Biol.* **6**, 253-260.
- Dill, K. A. (1990). Dominant forces in protein folding. *Biochemistry*, **29**, 7133-7155.
- Dobson, C. M. (1994). Protein folding. Solid evidence for molten globules. *Curr. Biol.* **4**, 636-40.
- Dobson, C. M. & Karplus, M. (1999). The fundamentals of protein folding: bringing together theory and experiment. *Curr. Opin. Struct. Biol.* **9**, 92-101.
- Doig, A. J. & Sternberg, M. J. (1995). Side-chain conformational entropy in protein folding. *Protein Sci.* **4**, 2247-2251.
- Donati, C., Glotzer, S. C. & Poole, P. H. (1999). Growing spatial correlations of particle displacements in a simulated liquid on cooling toward the glass transition. *Phys. Rev. Letters*, **82**, 5064-5067.
- Duval, F. P., Porion, P. & Van Damme, H. (1999). Microscale and macroscale diffusion of water in colloidal gels. A pulsed field gradient and NMR imaging investigation. *J. Phys. Chem. ser. B*, **103**, 5730-5735.
- Frauenfelder, H., Sligar, S. G. & Wolynes, P. G. (1991). The energy landscapes and motions of proteins. *Science*, **254**, 1598-1603.
- Gast, K., Zirwer, D., Muller-Frohne, M. & Damaschun, G. (1998). Compactness of the kinetic molten globule of bovine alpha-lactalbumin: a dynamic light scattering study. *Protein Sci.* **7**, 2004-2011.
- Griko, Y. V. & Remeta, D. P. (1999). Energetics of solvent and ligand-induced conformational changes in alpha-lactalbumin. *Protein Sci.* **8**, 554-561.
- Guo, Z. & Thirumalai, D. (1996). Kinetics and thermodynamics of folding of a *de novo* designed four-helix bundle protein. *J. Mol. Biol.* **263**, 323-343.
- Hendrix, T. M., Griko, Y. & Privalov, P. (1996). Energetics of structural domains in alpha-lactalbumin. *Protein Sci.* **5**, 923-931.
- Higgins, J. S. & Benoit, H. C. (1994). *Polymers and Neutron Scattering. Oxford Series on Neutron Scattering in Condensed Matter* (Lovesey, S. W. & Mitchell, E. W. J., eds), Clarendon Press, Oxford.
- Ichiye, T. & Karplus, M. (1991). Collective motions in proteins: a covariance analysis of atomic fluctuations in molecular dynamics and normal mode simulations. *Proteins: Struct. Funct. Genet.* **11**, 205-217.
- Karplus, M. & McCammon, J. A. (1983). Dynamics of proteins: elements and function. *Annu. Rev. Biochem.* **52**, 263-300.
- Karplus, M., Ichiye, T. & Pettitt, B. M. (1987). Configurational entropy of native proteins. *Biophys. J.* **52**, 1083-1085.
- Kataoka, M., Kuwajima, K., Tokunaga, F. & Goto, Y. (1997). Structural characterization of the molten globule of alpha-lactalbumin by solution X-ray scattering. *Protein Sci.* **6**, 422-430.
- Kataoka, M., Ferrand, M., Goupil-Lamy, A. V., Kamikubo, H., Yunoki, J., Oka, T. & Smith, J. C. (1999). Dynamical and structural modifications of staphylococcal nuclease on C-terminal truncation. *PHYSICA B*, **266**, 20-26.
- Kleifhaber, T., Labhardt, A. M. & Baldwin, R. L. (1995). Direct NMR evidence for an intermediate preceding

- the rate-limiting step in the unfolding of ribonuclease A. *Nature*, **375**, 513-515.
- Kuwajima, K. (1996). The molten globule state of alpha-lactalbumin. *Faseb J.* **10**, 102-109.
- Levitt, M., Gerstein, M., Huang, E., Subbiah, S. & Tsai, J. (1997). Protein folding: the endgame. *Annu. Rev. Biochem.* **66**, 549-579.
- Liu, R., Baase, W. A. & Matthews, B. W. (2000). The introduction of strain and its effects on the structure and stability of T4 lysozyme. *J. Mol. Biol.* **295**, 127-145.
- Lockless, S. W. & Ranganathan, R. (1999). Evolutionarily conserved pathways of energetic connectivity in protein families. *Science*, **286**, 295-299.
- Makhatadze, G. I. & Privalov, P. L. (1995). Energetics of protein structure. *Advan. Protein Chem.* **47**, 307-425.
- Matthews, B. W. (1995). Studies on protein stability with T4 lysozyme. *Advan. Protein. Chem.* **46**, 249-278.
- Peng, Z. Y. & Kim, P. S. (1994). A protein dissection study of a molten globule. *Biochemistry*, **33**, 2136-2141.
- Peng, Z. Y., Wu, L. C., Schulman, B. A. & Kim, P. S. (1995). Does the molten globule have a native-like tertiary fold?. *Philos. Trans. Roy. Soc. London B. Biol. Sci.* **348**, 43-47.
- Pike, A. C., Brew, K. & Acharya, K. R. (1996). Crystal structures of guinea-pig, goat and bovine alpha-lactalbumin highlight the enhanced conformational flexibility of regions that are significant for its action in lactose synthase. *Structure*, **4**, 691-703.
- Ptitsyn, O. B. (1995). Molten globule and protein folding. *Advan. Protein. Chem.* **47**, 83-229.
- Reat, V., Patzelt, H., Ferrand, M., Pfister, C., Oesterhelt, D. & Zaccai, G. (1998). Dynamics of different functional parts of bacteriorhodopsin: H-2H labeling and neutron scattering. *Proc. Natl Acad. Sci. USA*, **95**, 4970-4975.
- Receveur, V., Calmettes, P., Smith, J. C., Desmadril, M., Coddens, G. & Durand, D. (1997). Picosecond dynamical changes on denaturation of yeast phosphoglycerate kinase revealed by quasielastic neutron scattering. *Proteins: Struct. Funct. Genet.* **28**, 380-387.
- Redfield, C., Schulman, B. A., Milhollen, M. A., Kim, P. S. & Dobson, C. M. (1999). Alpha-lactalbumin forms a compact molten globule in the absence of disulfide bonds. *Nature Struct. Biol.* **6**, 948-952.
- Richards, F. M. (1977). Areas, Volumes, packing, and protein structure. *Ann. Rev. Biophys. Bioeng.* **6**, 151-176.
- Richards, F. M. & Lim, W. A. (1993). An analysis of packing in the protein folding problem. *Quart. Rev. Biophys.* **26**, 423-498.
- Schulman, B. A., Kim, P. S., Dobson, C. M. & Redfield, C. (1997). A residue-specific NMR view of the non-cooperative unfolding of a molten globule. *Nature Struct. Biol.* **4**, 630-634.
- Shortle, D. (1996). The denatured state (the other half of the folding equation) and its role in protein stability. *FASEB J.* **10**, 27-34.
- Smith, J. C. (1991). Protein dynamics: comparison of simulations with inelastic neutron scattering experiments. *Quart. Rev. Biophys.* **24**, 227-291.
- Volino, F. & Dianoux, A. J. (1980). Neutron incoherent scattering law for diffusion in a potential of spherical symmetry: general formalism and application to diffusion inside a sphere. *Mol. Phys.* **41**, 271-279.
- Wilson, G., Hecht, L. & Barron, L. D. (1996). The native-like tertiary fold in molten globule alpha-lactalbumin appears to be controlled by a continuous phase transition. *J. Mol. Biol.* **261**, 341-347.
- Windsor, C. (1981). *Pulsed Neutron Scattering*, Taylor & Francis Halsted Press, New York, London.
- Wright, P. E. & Dyson, H. J. (1999). Intrinsically unstructured proteins: re-assessing the protein structure-function paradigm. *J. Mol. Biol.* **293**, 321-331.
- Wu, L. C. & Kim, P. S. (1998). A specific hydrophobic core in the alpha-lactalbumin molten globule. *J. Mol. Biol.* **280**, 175-182.
- Wu, L. C., Peng, Z. Y. & Kim, P. S. (1995). Bipartite structure of the alpha-lactalbumin molten globule. *Nature Struct. Biol.* **2**, 281-286.
- Zaccai, G. (2000). How soft is a protein? A protein dynamics force constant measured by neutron scattering. *Science*, **288**, 1604-1607.

Edited by P. E. Wright

(Received 24 March 2000; received in revised form 20 June 2000; accepted 21 June 2000)